Standing out the key role of ultramicroporosity to tailor biomass-derived carbons for CO_2 capture

Nausika Querejeta, María Victoria Gil, Covadonga Pevida, Teresa A. Centeno[1]

Instituto Nacional del Carbón (INCAR-CSIC). Francisco Pintado Fe 26. 33011 Oviedo (Spain)

Abstract.

The successful tailoring of the ultramicroporosity remarkably increases the CO_2 uptake capacity of low cost-carbons derived by a simple one-pot physical activation of olive stones, coffee grounds, almond shells and grape seeds. A porous network dominated by ~40-46% of ultramicropores below 0.5 nm and no significant presence of pores above 0.7 nm boosts the CO_2 uptake at 1 bar and 298 K around 40% compared to materials with similar micropore volume. A slight ultramicropore widening causes the drop to a standard pattern that depends mainly on the micropore volume.

The detailed analysis of the CO_2 isotherms within the Dubinin´s theory provides simple clues for the optimization of carbons for CO_2 capture at ambient temperature and atmospheric pressure. Thus, a general pattern of around 7.2 mmol of CO_2 captured per cm^3 of ultramicropores is found for a variety of activated carbons and carbide derived-carbons with characteristic energy E_o of 29-22 kJ/mol. This feature is typical of materials with average micropore sizes from 0.65 to 1 nm. An enhancement of up to 10 mmol CO_2/cm^3 is achieved by carbons with E_o ranging between 30 and 32 kJ/mol which correlates with an extremely homogeneous porosity with average dimensions around 0.5 nm.

The excellent fit of the present carbons into general patterns exclusively based on the textural features reveals no significant influence of their surface functionalities on the CO_2 adsorption performance.

Keywords: CO_2 capture, adsorption, ultramicroporosity, activated carbon, biomass waste,

[1] Corresponding author. *E-mail address:* teresa@incar.csic.es; Tel.: +34 98 5119090 (T.A. Centeno)

1. Introduction

Although porous carbons present many advantages as adsorbents for CO_2 capture, they still face numerous scientific and technological challenges to turn into a real application [1-5]. In the last few years, tremendous efforts have been made in order to increase the capacity of carbons for CO_2 adsorption. The process essentially responds to the micropore-volume filling by physical adsorption although the CO_2 uptake can be enhanced chemisorption on surface sites. In this context, the current strategy focuses primarily on the development of advanced materials with a tailored porous structure and/or a doped surface [1,3, 5-19].

The industrial implementation of technologies for CO_2 capture appears to be much more sensitive to price than to performance and, therefore, the above goal must be achieved in parallel with costs reduction. Novel carbons with much higher CO_2 uptake might find a market but there is also an opportunity for activated carbons with comparable performance to those already existing but at a lower cost. In this context, the recycling of biomass wastes has received increasing attention in recent years [5,10,13,18,20-25]. Their use as precursors for the production of porous carbons offers significant potential for reducing both the total costs of capture and the environmental impact resulting from uncontrolled disposal of residues.

The current widespread approaches prioritize a maximum porosity development and, indeed, highly porous carbons with excellent CO_2 capture capacities have been successfully developed from biomass at laboratory scale. However, in most cases, they are prepared via multi-step processes involving hazardous activating agents and a variety of side reagents such as solvents, bases, acids, catalysts, etc. [10,13,18,20,23-27]. Such complexity hinders their implementation to large-scale sorbent production as much harmful residues are generated per carbon mass.

The present study suggests one-step physical activation of biomass wastes as a simple and more environmentally benign alternative for the preparation of sustainable carbons that in turn are competitive in terms of performance/cost ratio. Despite limited porosity, carbons from olive stones, coffee grounds, almond shells and grape seeds reach CO_2 uptakes between 2 and 3 mmol/g under conventional operational conditions widely used for comparison purposes in post-combustion CO_2 capture by means of adsorption (1 bar and 298 K). Such an enhancement in CO_2 adsorption is due, as will be shown herein, to a finely tailored ultramicroporosity.

The low CO_2 partial pressures associated to real post-combustion capture conditions imply that only those adsorbents with a significant presence of micropores will be able to retain significant amounts of CO_2 whereas the impact of larger pores appears to be

negligible [26,28,29]. On the basis of the determination of micropore size distributions, different studies have reported linear correlations between the CO_2 retention at low pressure and the volume of pores of a certain size [10,11,24,25,28,29]. However, the fact that the various relationships differ between types of carbons suggests that a more general description is needed. With the help of a detailed study of the textural characteristics of the present materials, relevant insights for the enhancement of CO_2 adsorption by carbons are provided.

2. Experimental

2.1. Materials

This study deals with activated carbons derived from a variety of biomass wastes: olive stones, coffee grounds, almond shells and grape seeds (Table 1). The latter was used after mechanical extraction of high-value oil. The synthesis procedure of the biomass-based carbons has been detailed elsewhere [30,31]. Basically, they were produced by simultaneous carbonization/activation under CO_2. Olive stones samples were also treated with 3 %v/v of O_2 in N_2. These activating agents have been selected for their simplicity and as standard reference in physical activation.

In the case of the use of grape seeds as precursors, the treatment was carried at 1073 K for 30 min. The synthesis of MH800 also involved a prior hydrothermal carbonization (HTC) at 473 K for 12 h. Diverse post-treatments such as heating at 1273 K, acid treatment, impregnation with diethylenetriamine (DETA) were carried on selected activated carbons in order to modify surface functionalities [30]. The different processes are compiled in Table S1.

2.2. Textural and chemical characterization

As the process of CO_2 capture at low pressures involves, exclusively, the narrower micropores, special care was taken in the structural characterization by standard CO_2 adsorption, typically performed up to relative pressure $p/p_S \sim 0.030$ at 273 K (Micromeritics TriStar 3000). The analysis of the CO_2 isotherms by the Dubinin´s theory provided the volume W_o of the so-called ultramicroporosity (< 1 nm) as well as the characteristic energy E_o. The latter is related to the average width of the corresponding micropores by $L_o = 10.8/(E_o-11.4)$. Following a simple geometrical correlation, the surface area of the narrow micropores was obtained by $S_{mi}=2000W_o/L_o$ [32].

The Non-Local Density Functional Theory (NLDFT) [33] has also been addressed as far as the determination of the total micropore volume (V_{NLDFT}) and the volume of micropores with a certain size are concerned. With some exceptions, the resulting cumulative pore volume and surface area agree with W_o and S_{mi}.

N_2 adsorption at 77 K (Micromeritics ASAP 2010) was also accomplished to get complementary data including larger micropores [29,34]. Its analysis by the standard approach based on BET equation led to the total surface area S_{BET}.

The different textural parameters were cross-checked by the NLDFT-analysis of CO_2 isotherm whereas Quenched Solid State Functional Theory (QSDFT) was used for N_2 adsorption [33]. In both cases, slit-shaped pores were assumed.

The carbon, hydrogen, and nitrogen contents were determined in a LECO CHNS-932 analyzer and the oxygen content in a LECO VTF-900 analyzer.

Temperature programmed desorption (TPD) tests were run in a thermogravimetric analyzer, Setaram TGA92, coupled to an OmnistarTM mass spectrometer-Pfeiffer Vacuum. They entailed heating the sample at 15 °C/min from room temperature to 1000 °C in argon flow (50 cm^3/min). The evolution of H_2O, CO and CO_2 was estimated by monitoring the mass to charge (m/z) values of 18, 28 and 44 in the mass spectrometer, the resulting curves being fitted with GaussianAmp peaks [30].

2.3. Assessment of the CO_2 capture capacity

CO_2 adsorption isotherms up to 1 bar at 298 K were measured in a TriStar 3000 from Micromeritics to gather information on capture capacity at low partial pressures (10^{-5}-0.035). In addition, CO_2 capture tests were performed in a thermogravimetric analyser (Setaram TGA92). After drying the materials at 373 K for 1 hour, the CO_2 uptakes at atmospheric pressure and 298 K were determined from the maximum mass increase of the sample when exposed to a pure CO_2 atmosphere. It was corroborated that both gravimetric and volumetric devices deliver similar data at 1 bar and 298 K.

For comparison purposes, advanced carbons, specifically synthetized from carbides (Skeleton Technologies) to cover the entire range of porosity, were also examined under the same experimental conditions. CDC-1 has an essentially microporous structure, CDC-2 and CDC-3 display micro- and mesopores and, finally, CDC-4 is mostly mesoporous (Fig. S1 and Table S2). The study was complemented by data (Table S3) from a selection of monolithic and powdered activated carbons from phenolic resins [28].

3. Results and Discussion

As summarized in Table 1, one-pot physical activation is able to develop highly microporous carbons from a variety of biomass waste sources. The selection of the precursor and the control of the preparation conditions lead to materials with surface areas of 680-1109 m^2/g, as measured by CO_2 adsorption at 273 K. The fact that these values surpass those obtained by the standard characterization based on the

adsorption of N_2 at 77 K provides a first indication of the essentially ultramicroporous structure of most of these materials [34]. The pore size distributions (PSD) obtained from the NLDFT-analysis of CO_2 isotherm complemented by QSDFT-data from N_2 adsorption confirm a major contribution from pores below 0.7 nm (Fig. 1). Such a narrow ultramicropore size distribution is rarely observed in carbons produced by activation or even by more sophisticated procedures such as nanotemplating [10,11,14,15,24,26,29,35,36].

Biomass Waste	Sample	n	W_o (cm^3g^{-1})	E_o (kJ/mol)	L_o (nm)	S_{mi} (m^2/g)	S_{BET} (m^2/g)	CO_2 uptake (mmol/g) [0.15 bar, 298 K]
Olive stones	RN1	2	0.21	32.13	0.52	746	514	0.88
	RN1P	2	0.22	29.65	0.59	745	281	-
	RN1A	2	0.21	31.88	0.53	738	348	-
	RN1PA	2	0.22	30.38	0.57	736	253	-
	RN2	1.7	0.44	24.94	0.80	1109	1248	0.99
	RN2-D5	1.8	0.38	24.72	0.81	938	1035	-
	RN2-D10	1.8	0.35	23.75	0.87	826	1014	-
Coffee	RN5	2	0.25	31.64	0.53	899	534	1.11
	RN5P	2	0.20	30.93	0.55	680	66	-
Almond shells	RN3	1.65	0.34	27.93	0.65	1001	847	0.98
Grape seeds	M800	2	0.23	31.89	0.53	819	535	0.91
	MH800	2	0.27	30.37	0.57	947	362	0.91
	M900	1.85	0.34	24.26	0.83	819	840	0.75

Table 1. Textural properties of the biomass based-activated carbons and CO_2 capture capacity under flue-gas conditions

It is observed that biomass is very sensitive to the operational conditions of the physical activation. For instance, the heating of olive stones under CO_2 flow leads to carbon RN2 which has marginally the highest pore volume and surface area (Table 1) whereas the treatment with 3 %v/v O_2/N_2 (RN1) favours the formation of smaller and narrowly distributed micropores (Fig. 1).

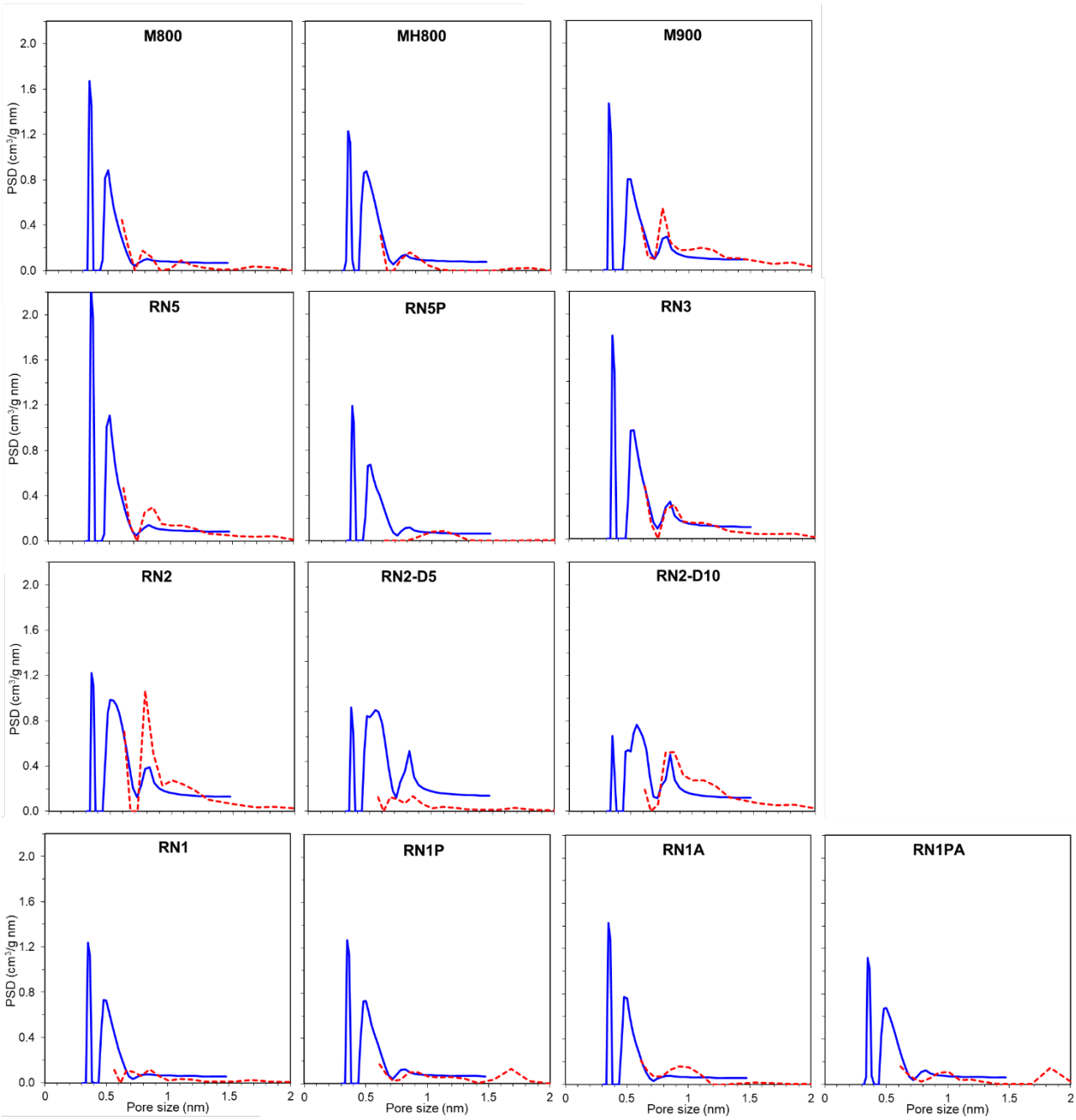

Figure 1. Pore size distribution of the activated carbons obtained by physical activation of biomass wastes. NLDFT analysis of CO_2 adsorption (------) and QSDFT analysis of N_2 adsorption (------) are combined.

On the other hand, the activation of grape seeds at 1073 and 1173 K yields samples M800 and M900, respectively, with equal specific surface area (Table 1). However, a simple increase of 100 K in temperature results in higher micropore volume and wider PSD. Whereas the porosity of M800 (0.23 cm^3/g) is virtually dominated by micropores below 0.7 nm and has hardly any pores above 0.9 nm, M900 also displays larger pores up to 1.8 nm (Fig. 1).

The little impact of further treatments on the textural characteristics reveals the strength of the porous network of the present biomass-based carbons. Thus, the structure of RN1 remains virtually unchanged, regardless of post-heating at 1273 K (RN1P), acid washing (RN1A) or the combination of both (RN1PA). The impregnation of RN2 with 5 and 10 wt.% of DETA (RN2-D5 and RN2-D10, respectively) appears to result in an amine film that partially blocks the porosity but the reduction in the volume available for CO_2 capture does not exceed 20% (Table 1). Fig. 1 confirms that the contribution from ultramicroporosity prevails and PSD seems little modified. In view of the textural characteristics of RN5P, the same applies for RN5 whose porosity is not affected significantly by thermal treatment at 1273 K.

Even though post-treatments have limited influence on porosity, the composition of the materials is modified as indicated by the contents of O and N summarized in Table S1. The impact on the surface chemistry is also revealed by the significant differences in the relative amounts of the major O-groups such as carbonyl and quinone, pyrone and chromene, carboxylic and lactone.

Since flue gas from coal-fired power stations typically contains 15 vol.% CO_2 at a pressure around 1 bar [3,18], the amount of CO_2 adsorbed at 0.15 bar and 298 K is an indicator of the potential of the materials as adsorbents in post-combustion CO_2 capture.

Despite the limited micropore volume of the present biomass waste-based activated carbons (0.2-0.4 cm^3/g), their uptakes at 0.15 bar and 298 K are around 0.9-1.1 mmol CO_2/g (Table 1). These values are close to 1.2 mmol/g, reported as the best performance for un-doped carbons under similar conditions [8-16,25]. As comparison, the capacity of the advanced carbide-derived carbons with S_{BET} of 1400-2000 m^2/g is significantly lower and only the essentially microporous CDC-1 results somewhat competitive with 0.85 mmol CO_2/g (Table S2).

The interest of the present biomass-derived carbons is confirmed by the attractive 2-3 mmol CO_2/g captured at 1 bar and 298 K (Fig. 2), which meet the upper-bound value of around 2.3-2.5 mmol/g reported for typical activated carbons under similar conditions [18, 28].

The increase in CO_2 uptake with the total micropore volume estimated by NLDFT-analysis of the CO_2 isotherm (V_{NLDFT}) suggests a specific contribution of the micropores to the capture process (Fig. 2a) although no clear proportionality is found. The same applies to the trend of CO_2 adsorbed *vs* tthe volume in ultramicropores below 0.8 nm (Fig. 2b). For instance, a similar uptake of ~2.4 mmol CO_2/g is achieved by activated carbons RN2-D10 and M800 and the carbide-derived carbons CDC-2 and CDC-3 although their volume $V_{<0.8\ nm}$ ranges between 0.16 and 0.25 cm^3/g (Fig. 2b). A somewhat better correlation is found with volume of pores smaller than 0.6 nm but the data scattering is still remarkable. As seen in Fig. 2c, carbons with $V_{<0.6\ nm}$ around 0.12 cm^3/g achieve CO_2 uptakes between 2.0 and 2.7 mmol/g.

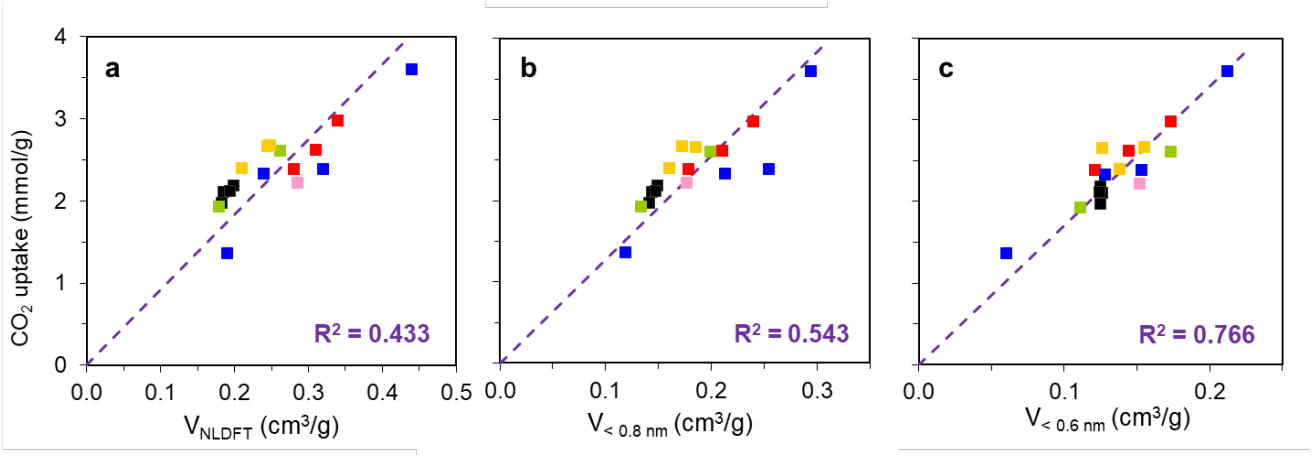

Figure 2. CO_2 uptake (298 K, 1 bar) by carbons *versus* total micropore volume (a); *versus* volume in pores smaller than 0.8 nm (b) and *versus* volume in pores smaller than 0.6 nm (c), as estimated by NLDFT
Series RN1 ■, RN2 ■, RN3 ■, RN5 ■, M ■ and CDC ■

Such relevant uncertainties indicate that this approach [10,11,24,25,29] cannot be applied straightforward to the search of an optimized carbon for CO_2 capture.
As shown in detail previously [28], the capture of CO_2 by carbons simply follows the Dubinin's theory. The mechanism is described by the Dubinin-Astakhov (D-A) equation which relates the degree of filling of micropores with the partial pressure and temperature:

$$W = W_o \exp[-(A/\beta E_o)^n] \quad \text{Eq. (1)}$$

where W (cm^3/g) is the volume adsorbed at temperature T (K) and relative pressure p/p_o, W_o (cm^3/g) is the micropore volume, $A = RTln(p_o/p)$, β is a scaling factor depending on the adsorbate (0.36 for CO_2) and E_o (kJ/mol), is the so-called characteristic energy of the adsorbent. Therefore, reliable predictions for CO_2 uptake at any pressure and temperature can be made.

Systematic studies by vapour adsorption and on immersion calorimetry [32] showed that n=2, which corresponds to the Dubinin-Radushkevich (D-R) equation, reflects an intermediate situation between monodisperse (n=3) and strongly heterogeneous micropore system (n< 2).

The analysis of the CO_2 adsorption isotherms at 273 K of the present carbons by means of the linearization of the D-A equation leads to the corresponding W_o and E_o (Table 1). The majority of the present carbons fit the D-R equation over a wide range of relative pressures (Fig. 3a displays some relevant examples) which means that their porosity essentially consists of uniform micropores. By contrast, the curvature of the D−R plots corresponding to the samples RN2, RN3 and M900 (Fig. 3b) reveals heterogeneous microporosity. For these carbons the linearization is reached by using values of n of 1.65-1.8 (Table 1).

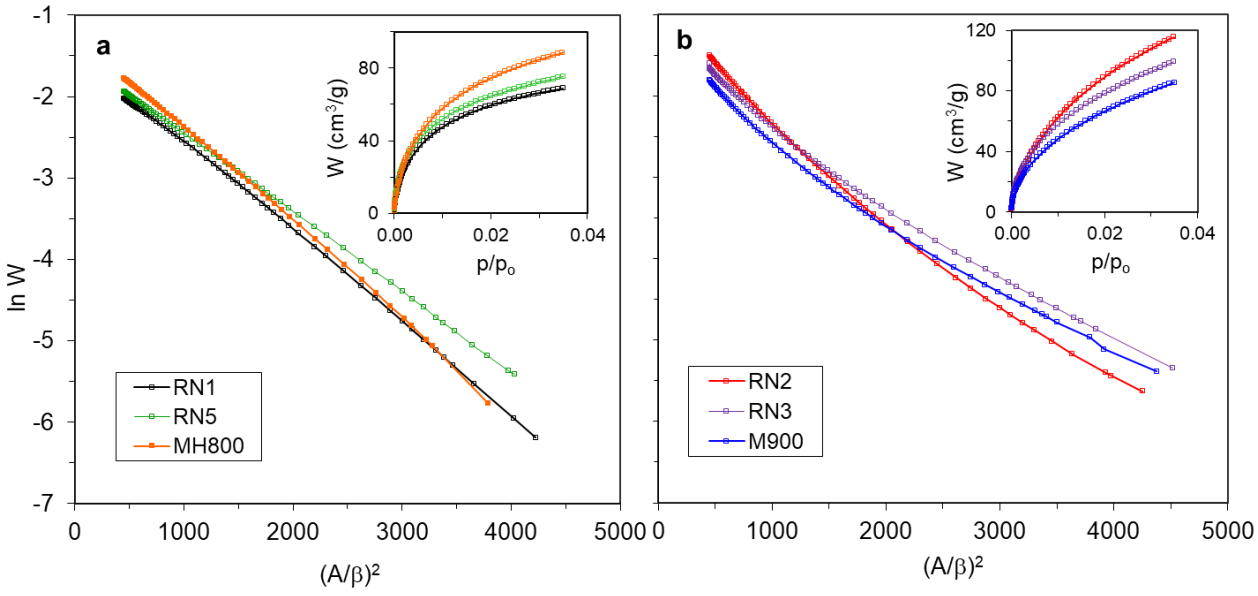

Figure 3. D-R plot for the adsorption of CO_2 at 273 K by different biomass-based activated carbons. Inset: Isotherms

The relationship between the CO_2 uptake at 1 bar and 298 K and the total micropore volume estimated by the Dubinin´s theory (Fig. 4) is used as basis to assess the carbons characteristics responsible of the CO_2 capture capacity under post-combustion conditions. Firstly, the overall trend found for a large variety of materials (shown by the straight line in Fig.4) highlights the contribution of the total volume of micropores (W_o) to the CO_2 retention. Secondly, the substantial gap of around 40% higher capacity achieved by carbons of series RN1, RN5 and the carbons M800 and MH800 compared to other materials with similar micropore volumes suggests the contribution from another parameter.

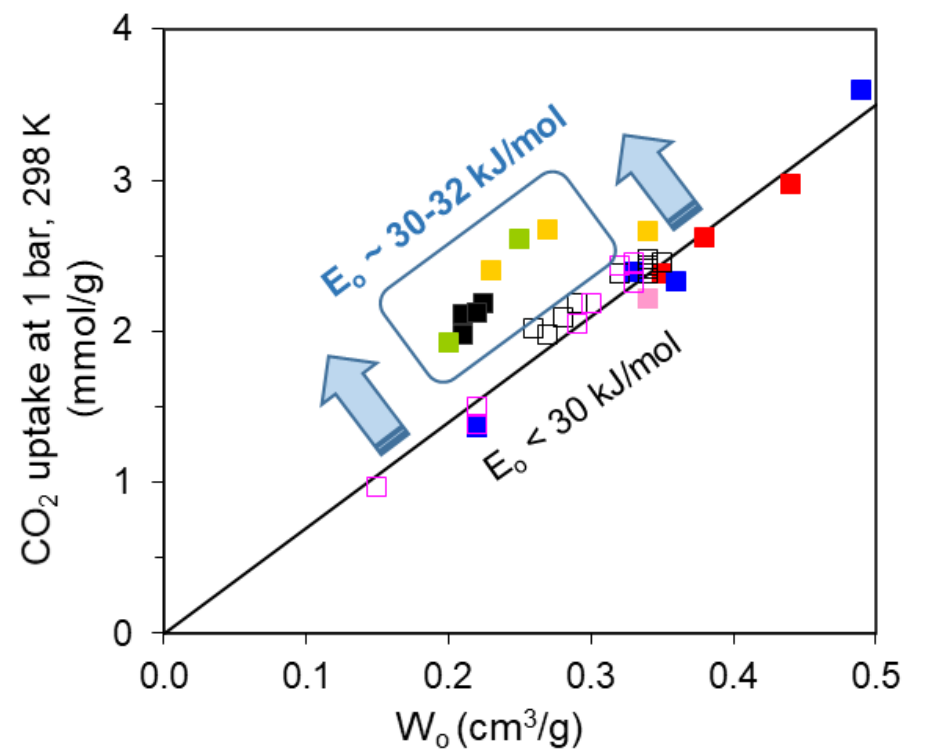

Figure 4. CO_2 uptake (298 K, 1 bar) by carbons *versus* the total micropore volume estimated by the Dubinin´s theory: Series RN1 ■, RN2 ■, RN3 ■, RN5 ■, M ■, CDC ■, activated carbon monoliths □ and activated carbons from phenolic resins □ [28].

In agreement with the D-A equation, the volume of micropores W_o is a key parameter, but the characteristic energy E_o is also of great concern. A deeper analysis of data in Table 1 reveals that the enhancement of the CO_2 uptake observed in Fig. 4 corresponds to carbons with E_o ranging between 30 and 32 kJ/mol. This is not surprising since such high values reveal a very narrow porosity with average dimensions around 0.5 nm [32] wherein the adsorption energy is increased by the overlapping of the potencial fields from the pore walls [11,32]. The standard pattern (represented by the black line in Fig.4) is followed by materials with E_o of 29-22 kJ/mol which precisely are typical of microporous carbons with average micropore sizes from 0.65 to 1 nm. It corresponds to around 7.2 mmol CO_2/cm^3 of micropore volume as proved by CO_2 adsorption at 273 K. However, when ultramicroporosity is tailored values of up to 10 mmol CO_2/cm^3 are attained.

The specific features of carbons contributing to each trend are qualitatively confirmed by the micropore size distributions determined by the analysis of the CO_2 isotherm by NLDFT.

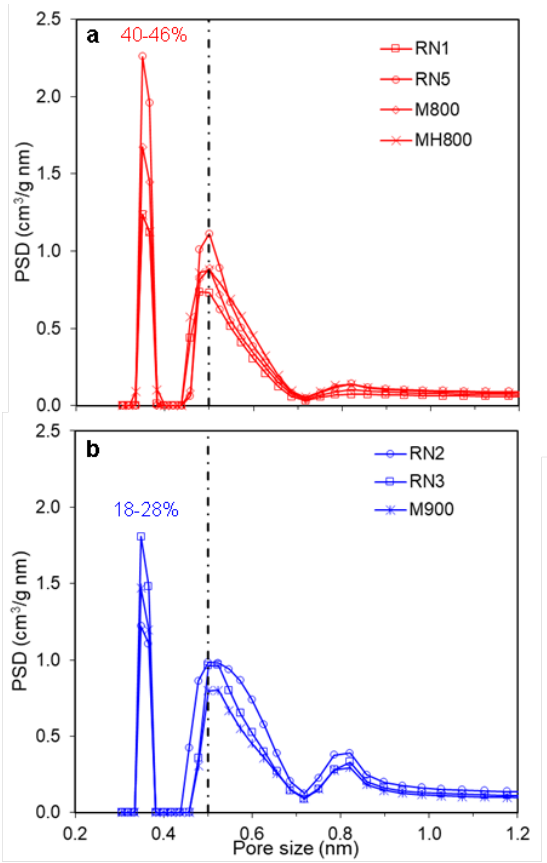

Figure 5. Micropore size distribution of biomass-derived activated carbons: (a) materials with enhanced CO_2 capture capacity and (b) those that follow the general pattern in Fig. 4.

It is observed that the increased CO_2 uptake of series RN1 and RN5 and of carbons M800 and MH800 correlates with their narrow PSDs dominated by 40-46% of ultramicropores below 0.5 nm (Fig. 5a). The drop of this percentage down to values of 18-28% in carbons of RN2- and RN3-series as well as in M900 (Fig. 5b) results highly detrimental to their capture capacity.

It is noteworthy that, despite M900 exhibits 50% higher micropore volume than M800, both materials attain similar uptakes of 2.7 and 2.4 mmol/g, respectively (Fig. 6a). Similarly, for sample RN2, which shows twice the volume of micropores of RN1, a capture capacity only 40% higher than RN1 was measured (Fig. 6b). The lower efficiency of M900 and RN2 results from the presence of slightly larger micropores which reduces the adsorption potential. This is illustrated in Fig. 6 (insets) where the fraction of CO_2 adsorbed by these samples at any given pressure is lower than for the respective counterparts M800 and RN1 with somewhat narrower porosity.

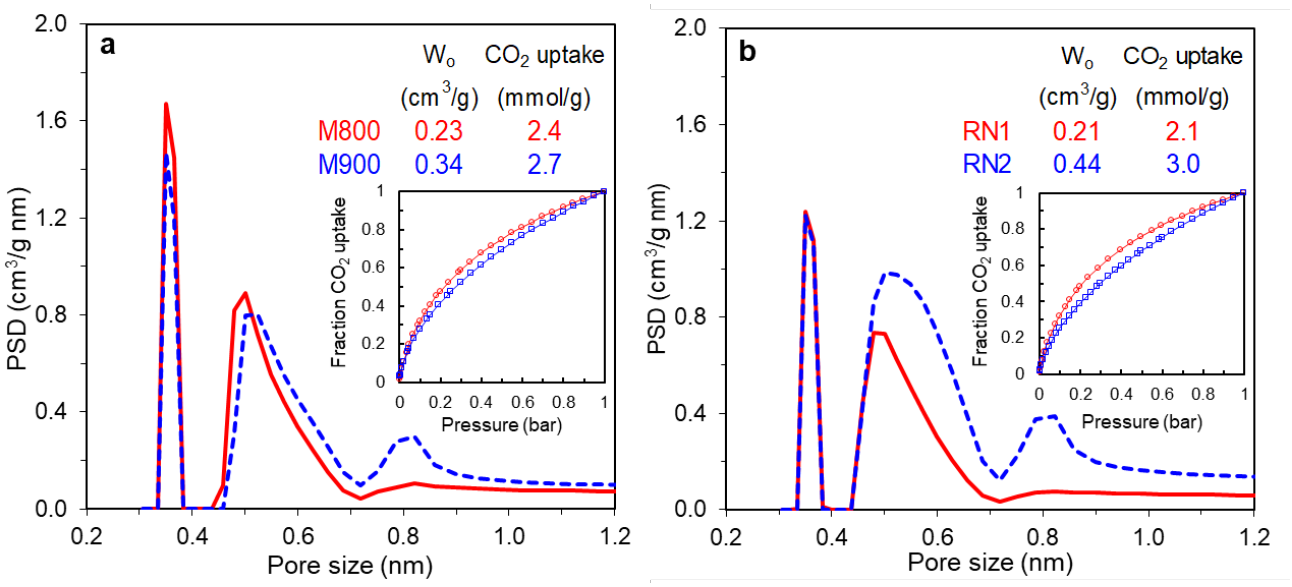

Figure 6. Effect of the micropore size distribution of carbons on their CO_2 uptake.

The excellent fit of all materials into the general profiles shown in Fig. 4 reveals the negligible influence of the surface functionalities on the CO_2 adsorption. Independently of their O and N contents (Table S1), the different sets of carbons follow similar patterns and the CO_2 retention is exclusively related to their values of W_o and E_o. For instance, the similar textural properties for samples of series RN1 are accompanied by comparable CO_2 uptake regardless of the different amount and nature of surface functionalities (Table S4).

Such result is in agreement with López-Ramón et al. [37] and Adeniran et al. [38] but not necessarily in contradiction with other studies reporting capture increases in the presence of heteroatoms [1,2,5-7,9,13,14,18]. It Indicates that the adsorption of CO_2 would be affected by the presence of specific surface functionalities. This issue is beyond the scope of the present study but it is being considered in other ongoing research.

4. Conclusions

As an alternative to the current widespread option that prioritizes a maximum development of the pore volume, this paper illustrates that the tailoring of the ultramicroporosity remarkably increases the ability of carbons to capture CO_2 at room temperature and atmospheric pressure.

Despite the simplicity of their synthesis route involving one-pot physical activation with no need for hazardous chemicals, low-cost carbons derived from biomass wastes reach CO_2 uptakes of 2-3 mmol/g at 1 bar and 298 K. These capacities meet the upper-bound of around 2.5 mmol/g found for typical activated carbons and other porous carbons under similar conditions.

A porous network dominated by ~40-46 % of ultramicropores below 0.5 nm and no significant presence of pores above 0.7 nm allows exceeding around 40% the CO_2 retention capability of materials with similar micropore volume. Minor differences in such a finely tailored ultramicroporosity impact the carbons efficiency.

With the help of the analysis of the CO_2 isotherms (273 K) within the Dubinin´s theory, a general correlation of around 7.2 mmol of CO_2 captured per cm^3 of ultramicropore volume is found. This pattern is followed by carbons with characteristic energy of 29-22 kJ/mol, which is that of typical microporous carbons with average micropore sizes from 0.65 to 1 nm. An enhancement of up to 10 mmol CO_2/cm^3 is reached by carbons with E_o ranging between 30 and 32 kJ/mol. Such high values of characteristic energy correlates with an extremely homogeneous porosity with average dimensions around 0.5 nm.

The surface functionalities of the present carbons do not affect their ability to adsorb CO_2.

Acknowledgements

N.Q. acknowledges a fellowship from the Gobierno del Principado de Asturias (Programa Severo Ochoa).

References

[1] Y. Zhao, X. Liu, Yu Han. Microporous carbonaceous adsorbents for CO_2 separation via selective adsorption. RSC Adv. 2015, 5, 30310-30330. DOI: 10.1039/c5ra00569h.

[2] B.P. Spigarelli, S.K. Kawatra. Opportunities and challenges in carbon dioxide capture. J. CO_2 Util. 2013, 1, 69–87. DOI:10.1016/j.jcou.2013.03.002

[3] T.C. Drage, C.E. Snape, L.A. Stevens, J.Wood, J.Wang, A. I. Cooper, R. Dawson, X. Guo, C. Satterley, R. Irons. Materials challenges for the development of solid sorbents for post-combustion carbon capture. J. Mater. Chem. 2012, 22, 2815-2823. DOI: 10.1039/C2JM12592G.

[4] H.A. Patel, J. Byun, C.T. Yavuz. Carbon Dioxide Capture Adsorbents: Chemistry and Methods. ChemSusChem 2017, 10, 1303-1317. DOI: 10.1002/cssc.201601545.

[5] J. Wang, L. Huang, R. Yang, Z. Zhang, J. Wu, Y. Gao, Q. Wang, D. O'Hare, Z. Zhong. Recent advances in solid sorbents for CO_2 capture and new development trends. Energy Environ. Sci. 2014, 7, 3478-3518. DOI: 10.1039/c4ee01647e.

[6] S.Y. Lee, S.J. Park. A review on solid adsorbents for carbon dioxide capture. J Indust Eng Chem. 2015, 23, 1-11. DOI: 10.1016/j.jiec.2014.09.001.

[7] Y. X., R. Mokaya, G.S. Walker, Y. Zhu. Superior CO_2 adsorption capacity on N-doped, high-surface-area, microporous carbons templated from zeolite. Adv. Energy Mater. 2011, 1, 678–683. DOI: 10.1002/aenm.201100061.

[8] A. Wahby, J.M. Ramos-Fernández, M. Martínez-Escandell, A. Sepúlveda-Escribano, J. Silvestre-Albero, and F. Rodríguez-Reinoso. High-surface-area carbon molecular sieves for selective CO_2 adsorption. ChemSusChem 2010, 3, 974-981. DOI: 10.1002/cssc.201000083.

[9] M. Nandi, K. Okada, A. Dutta, A. Bhaumik, J. Maruyama, D. Derks, H. Uyama. Unprecedented CO_2 uptake over highly porous N-doped activated carbon monoliths prepared by physical activation. Chem. Commun. 2012, 48, 10283-10285. DOI: 10.1039/c2cc35334b.

[10] H. Wei, S. Deng, B. Hu, Z. Chen, B. Wang, J. Huang, G. Yu. Granular bamboo-derived activated carbon for high CO_2 adsorption: The dominant role of narrow micropores. ChemSusChem 2012, 5, 2354-2360. DOI: 10.1002/cssc.201200570.

[11] Z. Zhang, J. Zhou, W. Xing, Q. Xue, Z. Yan, S. Zhuo, S.Z. Qiao, Critical role of small micropores in high CO_2 uptake. Phys. Chem. Chem. Phys. 2013, 15, 2523-2529. DOI: 10.1039/c2cp44436d.

[12] N. P. Wickramaratne, M. Jaroniec. Importance of small micropores in CO_2 capture by phenolic resin-based activated carbon spheres. J. Mater. Chem. A 2013, 1, 112-116. DOI: 10.1039/c2ta00388k.

[13] X. Fan, L. Zhang, G. Zhang, Z. Shu, J. Shi. Chitosan derived nitrogen-doped microporous carbons for high performance CO_2 capture. Carbon 61 (2013) 423-430. DOI: 10.1016/j.carbon.2013.05.026

[14] M. Saleh, J.N. Tiwari, K.C. Kemp, M. Yousuf, K.S. Kim. Highly selective and stable carbon dioxide uptake in polyindole-derived microporous carbon materials. Environ. Sci. Technol. 2013, 47, 5467–5473. DOI: 10.1021/es3052922.

[15] E. Masika, R. Mokaya. High surface area metal salt templated carbon aerogels via a simple subcritical drying route: preparation and CO2 uptake properties. RSC Adv. 2013, 3, 17677-17681. DOI: 10.1039/c3ra43420f.

[16] M. Saleh, V. Chandra, K. C. Kemp, K.S. Kim. Synthesis of N-doped microporous carbon via chemical activation of polyindole-modified graphene oxide sheets for selective carbon dioxide adsorption. Nanotechnology 2013, 24, 255702. DOI: 10.1088/0957-4484/24/25/255702.

[17] K. C. Kemp, V. Chandra, M. Saleh, K.S Kim. Reversible CO_2 adsorption by an activated nitrogen doped graphene/polyaniline material. Nanotechnology, 2013, 24, 235703. DOI10.1088/0957-4484/24/23/235703.

[18] N.A. Rashidi, S. Yusup. An overview of activated carbons utilization for the post-combustion carbon dioxide capture. J. CO_2 Util. 2016, 13, 1-16. DOI: 10.1016/j.jcou.2015.11.002.

[19] J. Zhou, Z. Li, W. Xing, H. Shen, X. Bi, T. Zhu, Z. Qiu, S. Zhuo. A new approach to tuning carbon ultramicropore size at sub-Angstrom level for maximizing specific capacitance and CO_2 Uptake. Adv. Funct. Mater. 2016, 26, 7955-7964. DOI: 10.1002/adfm.201601904.

[20] M. Olivares-Marín, M. Maroto-Valer. Development of adsorbents for CO_2 capture from waste materials: A review. Greenhouse Gas Sci Technol. 2012, 2, 20-35. DOI: 10.1002/ghg.45.

[21] A.S. González, M.G. Plaza, F. Rubiera, C. Pevida. Sustainable biomass-based carbon adsorbents for post-combustion CO_2 capture. Chem. Eng. J. 2013, 230, 456-465. DOI: 10.1016/j.cej.2013.06.118.

[22] A. Serge Ello, L.K.C. de Souza, A. Trokourey, M. Jaroniec. Coconut shell-based microporous carbons for CO_2 capture. Microporous Mesoporous Mater. 2013, 180, 280-283. DOI: 10.1016/j.jcou.2017.01.006.

[23] K. Chomiak, S. Gryglewicz, K. Kierzek, J. Machnikowski. Optimizing the properties of granular walnut-shell based KOH activated carbons for carbon dioxide adsorption. J. CO_2 Util. 2017, 21, 436-443. DOI: 10.1016/j.jcou.2017.07.026.

[24] J. Serafin, U. Narkiewicz, A.W. Morawski, R. J. Wróbel, B. Michalkiewicz. Highly microporous activated carbons from biomass for CO_2 capture and effective micropores

at different conditions. J. CO_2 Util. 2017, 18, 73-79. DOI: 10.1016/j.jcou.2017.01.006.
[25] S. Deng, H. Wei, T. Chen, B. Wang, J. Huang, G. Yu. Superior CO_2 adsorption on pine nut shell-derived activated carbons and the effective micropores at different temperatures. Chem. Eng. J. 2014, 253, 46-54.
[26] H.M. Coromina, D.A. Walsh, R. Mokaya. Biomass-derived activated carbon with simultaneously enhanced CO_2 uptake for both pre- and post-combustion capture applications. J. Mater. Chem. A, 2016, 4, 280-289. DOI: 10.1039/c5ta09202g.
[27] A.S. Ello, L.K.C. de Souza, A. Trokourey, M. Jaroniec. Development of microporous carbons for CO_2 capture by KOH activation of African palm shells. J. CO_2 Util. 2013, 2, 35-38. 0.1016/j.jcou.2013.07.003.
[28] C.F. Martín, M.G. Plaza, J.J. Pis, F. Rubiera, C. Pevida, T.A. Centeno. On the limits of CO_2 capture capacity of carbons. Sep. Purif. Technol. 2010, 74, 225-229.DOI: 10.1016/j.seppur.2010.06.009.
[29] V. Presser, J. McDonough, S.H. Yeon, Y. Gogotsi. Effect of pore size on carbon dioxide sorption by carbide derived carbon. Energy Environ. Sci., 2011, 4, 3059-3066. DOI: 10.1039/c1ee01176f.
[30] N. Querejeta, M.G. Plaza, F. Rubiera, C. Pevida. Water vapor adsorption on biomass based carbons under post-combustion CO_2 capture conditions: Effect of post-treatment. Materials 2016, 9, 359. DOI: 10.3390/ma9050359.
[31] N. Querejeta, M.V. Gil, F. Rubiera, C. Pevida. Sustainable coffee-based CO_2 adsorbents: toward a greener production via hydrothermal carbonization. Greenhouse Gas Sci Technol. 2017, 0, 1-15. DOI: 10.1002/ghg.1740.
[32] F. Stoeckli, in Porosity in carbons. Characterization and applications, ed. J. Patrick, Edward Arnold, London, 1995, Ch. 3, pp. 67–92.
[33] J. Landers, G.Y. Gor, A.V. Neimark. Density functional theory methods for characterization of porous materials. Colloids and Surfaces A: Physicochem. Eng. Aspects 2013, 437, 3-32. DOI: 10.1016/j.colsurfa.2013.01.007.
[34] B. Lobato, L. Suárez, L. Guardia, T.A. Centeno. Capacitance and surface of carbons in supercapacitors. Carbon 2017, 122, 434-445. DOI: 10.1016/j.carbon.2017.06.083.
[35] C. Hyo Kim, J.H. Wee, Y. A. Kim, K. Seung Yang, C.M. Yang. Tailoring the pore structure of carbon nanofibers for achieving ultrahigh-energy-density supercapacitors using ionic liquids as electrolytes. J. Mater. Chem. A, 2016, 4, 4763-4770. DOI: 10.1039/c5ta10500e.
[36] H. Itoi, H. Nishihara, T. Kogure, T. Kyotani. Three-Dimensionally Arrayed and Mutually Connected 1.2-nm Nanopores for High-Performance Electric Double Layer Capacitor. J. Am. Chem. Soc. 2011, 133, 1165-1167. DOI:10.1021/ja108315p.

[37] M.V. López-Ramón, F. Stoeckli, C. Moreno-Castilla, F. Carrasco-Marín. Specific and nonspecific interactions between methanol and ethanol and active carbons. Langmuir 2000, 16, 5967-5972. DOI: 10.1021/la991352q.
[38] B. Adeniran, R Mokaya. Is N-doping in porous carbons beneficial for CO_2 storage? Experimental demonstration of the relative effects of pore size and N-doping. Chem. Mater. 2016, 28, 994-1001. DOI: 10.1021/acs.chemmater.5b05020.

Supplementary Information

Standing out the key role of ultramicroporosity to tailor biomass-derived carbons for CO_2 capture

Nausika Querejeta, María Victoria Gil, Covadonga Pevida, Teresa A. Centeno[2]

Instituto Nacional del Carbón (INCAR-CSIC). Francisco Pintado Fe 26. 33011 Oviedo (Spain)

[2] Corresponding author. *E-mail address:* teresa@incar.csic.es; Tel.: +34 98 5119090 (T.A. Centeno)

Table S1. Synthesis conditions and chemical features of the activated carbons from biomass wastes

Biomass	Sample	Pre-treatment	Activating agent	Activation conditions	Post-treatment	Elemental analysis	
						N (wt.%)	O (wt.%)
Olive stones	RN1	–	3 vol% O_2/N_2	923 K-5.5 h	–	0.4	7.4
	RN1P	–			N_2 1273 K-30 min [30]	0.6	4.2
	RN1A	–			1M HCl [30]	0.4	9.9
	RN1PA	–			N_2 1273 K-30 min + 1M HCl [30]	0.3	14.2
	RN2	–	CO_2	1073 K-6 h	–	0.7	11.3
	RN2-D5	–			Impregnation with 5% DETA [30]	1.3	11.6
	RN2-D10	–			Impregnation with 10 % DETA [30]	3.8	13.4
Coffee	RN5	–	CO_2	973 K-8 h	–	4.1	12.2
	RN5P	–			N_2 at 1273 K-30 min [31]	3.1	6.3
Almond shells	RN3	–	CO_2	1023 K-4 h	–	1.3	16.8
Grape seeds	M800	–		1073 K-30 min	–	1.8	12.9
	MH800	HTC 473 K-12 h		1073 K-30 min	–	2.2	7.8
	M900	–		1173 K-30 min	–	2.1	15.3

Figure S1. Pore size distribution of carbide derived-carbons obtained from NLDFT analysis of CO_2 adsorption (------) and QSDFT analysis of N_2 adsorption (------)

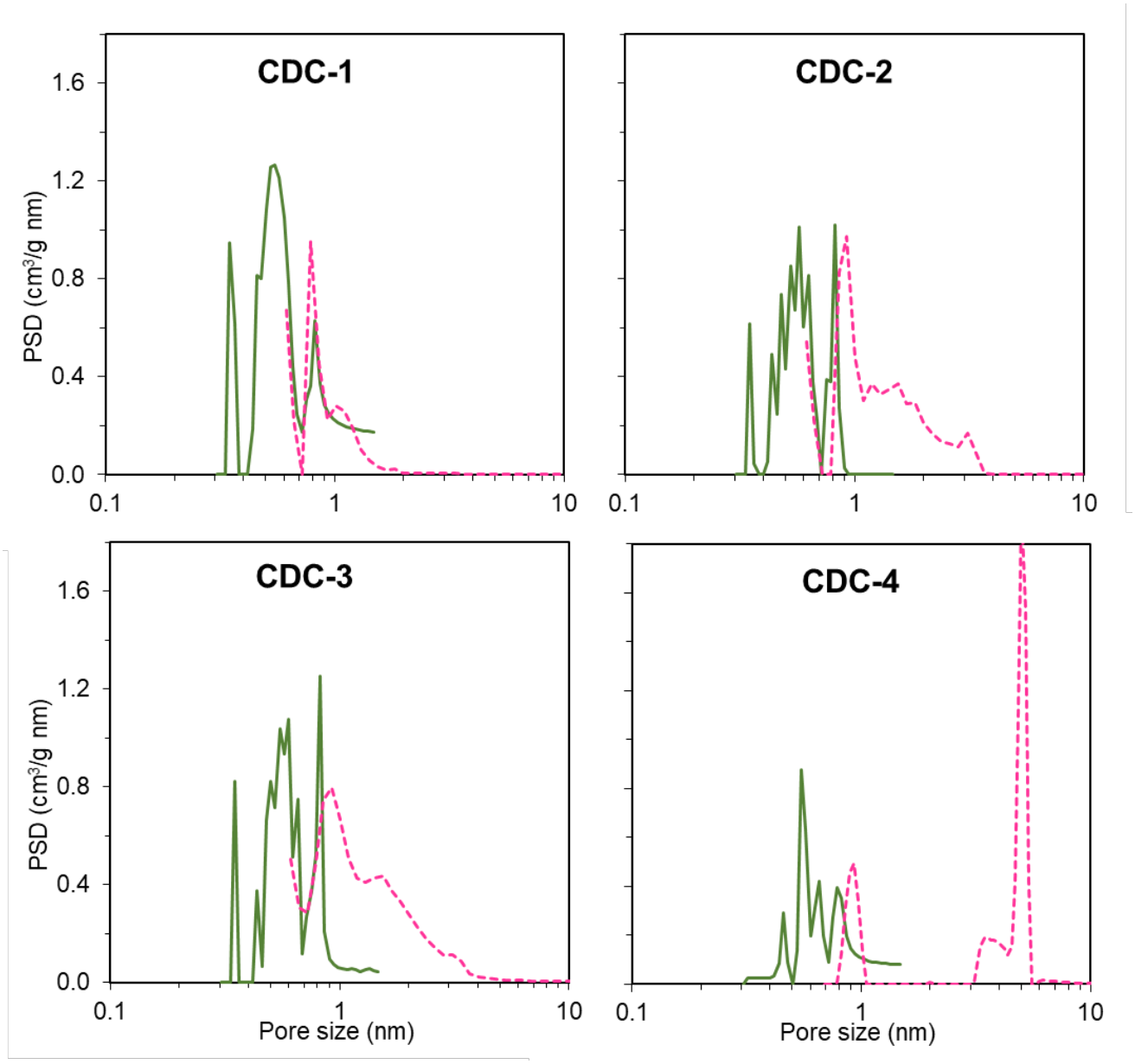

Table S2. Textural features and CO_2 capture of the carbide derived-carbons

Sample	W_o (cm^3/g)	E_o (kJ/mol)	L_o (nm)	S_{mi} (m^2/g)	S_{BET} (m^2/g)	CO_2 uptake (mmol/g) (0.15 bar, 298 K)
CDC-1	0.49	26.14	0.73	1349	1397	0.85
CDC-2	0.36	24.67	0.81	874	1787	0.48
CDC-3	0.33	25.68	0.76	861	1978	0.56
CDC-4	0.22	22.48	0.98	451	1504	0.23

Table S3. Textural parameters of the phenolic-resin-derived activated carbons [1]

Carbon	N_2 (77 K) - adsorption								CO_2 (273 K) - adsorption			
	V_{tot} ($cm^3\ g^{-1}$)	W_o ($cm^3\ g^{-1}$)	E_o (kJ mol^{-1})	L_o (nm)	S_{mi} ($m^2\ g^{-1}$)	S_e ($m^2\ g^{-1}$)	S_{total} ($m^2\ g^{-1}$)	D_{KJS} (nm)	W_o ($cm^3\ g^{-1}$)	E_o (kJ mol^{-1})	L_o (nm)	S_{mi} ($m^2\ g^{-1}$)
M1	0.35	0.33	27.7	0.66	1000	10	710	-	0.34	28.0	0.65	1046
M2	0.55	0.51	22.9	0.94	1085	11	1105	-	0.34	27.3	0.68	1000
M3	0.60	0.54	22.0	1.02	1059	8	1200	-	0.34	26.8	0.70	971
M4	0.58	0.50	21.5	1.07	935	13	1190	-	0.29	27.0	0.69	840
M5	0.85	0.71	20.1	1.25	1136	6	1467	-	0.35	26.2	0.73	959
M6	1.50	0.36	21.0	1.12	643	269	909	5.2-54.0	0.26	29.5	0.59	881
M7	0.55	0.29	24.2	0.84	690	187	648	24.4	0.28	29.2	0.61	918
M8	0.71	0.45	22.8	0.95	947	140	961	26.5	0.34	27.5	0.67	1015
M9	0.85	0.64	20.2	1.23	1041	116	1472	29.7	0.32	26.3	0.72	889
M11	0.27	0.25	26.5	0.71	704	81	550	Broad PSD>10	0.27	29.5	0.57	877
M12	0.59	0.51	22.1	1.01	1010	110	1140	Broad PSD>10	0.33	26.7	0.71	930
GPFNA-20	0.30	0.29	24.3	0.84	690	2	755	-	0.30	27.3	0.68	882
CLC8A9-20	0.26	0.24	22.6	0.96	500	5	626	-	0.22	26.6	0.71	620
CLC8A9-40	0.61	0.51	18.8	1.45	703	6	1381	-	0.29	26.0	0.74	784
E1C7A75-16	0.31	0.31	24.1	0.85	729	2	781	-	0.32	27.8	0.66	970
E1C7A8-24	0.34	0.33	23.4	0.90	733	9	841	-	0.33	27.0	0.69	957
E1C7A8-41	0.56	0.51	20.8	1.15	887	15	1269	-	0.33	26.2	0.73	904
PE1C8A9-20	0.17	0.12	21.5	1.07	224	7	306	2.5-7.1	0.15	26.6	0.71	423
PE1C8A9-27	0.29	0.22	21.0	1.12	393	15	553	7.6	0.22	25.2	0.78	564

Table S4. Amount of CO and CO_2 evolved during the temperature programmed desorption (TPD) experiments and distribution of surface oxygenated functionalities

Sample	CO	CO_2	Anhydride	Phenol	Carbonyl/Quinone	Pyrone/ Chromene	Carboxylic	Anhydride	Peroxide	Lactone
RN1	1438	884	–	–	380	620	100	–	470	300
RN1P	824	308	–	–	14	140	130	–	40	130
RN1A	3176	2645	137	–	1310	–	250	20	–	1850
RN1PA	–	–	–	–	–	–	–	–	–	–
RN2	2249	890	–	52	60	800	400	–	–	430
RN2D5	943	473	–	32	–	250	210	–	–	220
RN2D10	840	577	–	–	30	270	100	–	–	420
RN5	2541	1090	–	–	100	1500	360	–	–	609
RN5P	1329	310	–	–	98	507	106	–	27	163
RN3	2836	1170	–	–	119	1322	603	–	464	52
M800	1679	688	–	–	242	530	285	–	–	339
MH800	610	172	–	–	132	133	64	–	–	111
M900	2315	808	–	–	244	715	340	–	–	450

References

[1] C.F. Martín, M.G. Plaza, J.J. Pis, F. Rubiera, C. Pevida, T.A. Centeno. On the limits of CO_2 capture capacity of carbons. Sep. Purif. Technol. 2010, 74, 225-229.DOI: 10.1016/j.seppur.2010.06.009.